Size-changeable X-ray beam collimation using an adaptive X-ray optical system based on four deformable mirrors

T. Goto[a], S. Matsuyama[a], H. Nakamori[a,b], H. Hayashi[a], Y. Sano[a],
Y. Kohmura[c], M. Yabashi[c], T. Ishikawa[c], K. Yamauchi[a]
[a] Department of Precision Science and Technology, Graduate School of Engineering, Osaka University, 2-1 Yamada-oka, Suita, Osaka 565-0871, Japan
[b] JTEC Corporation, 2-4-35 Yamabuki, Saito, Ibaraki-city Osaka 567-0086, Japan
[c] RIKEN/SPring-8 Center, 1-1-1 Kouto, Sayo-cho, Sayo-gun, Hyogo 679-5148, Japan

ABSTRACT

A two-stage adaptive optical system using four piezoelectric deformable mirrors was constructed at SPring-8 to form collimated X-ray beams. The deformable mirrors were finely deformed to target shapes (elliptical for the upstream mirrors and parabolic for the downstream mirrors) based on shape data measured with the X-ray pencil beam scanning method. Ultraprecise control of the mirror shapes enables us to obtain various collimated beams with different beam sizes of 314 μm (358 μm) and 127 μm (65 μm) in the horizontal (vertical) directions, respectively, with parallelism accuracy of ~ 1 μrad rms.

Keywords: piezoelectric bimorph mirror, X-ray mirror, Kirkpatrick-Baez mirror optics, adaptive mirror

1. INTRODUCTION

Various X-ray analyses based on scattering, fluorescence, and photoelectrons are essential tools in the scientific and industrial areas. Moreover, recent intense and high-coherence X-rays generated by third-generation synchrotron radiation facilities enabled the analyses to be drastically improved. In the facilities, X-rays are usually shaped into a focused or divergent beam by refractive[1,2] and diffractive lenses[3] and mirrors[4,5] according to the sample size and experiments. Thus, the key elements have been developed and improved in the facilities to effectively utilize X-rays. On the other hand, storage-ring-based X-ray sources have also advanced to obtain ultra-low emittance, i.e., extremely high average brilliance and a high degree of transverse coherence. According to the SPring-8 II design report[6], the brilliance is expected to be improved 100 times more than with existing storage rings. With the increase in brilliance, one sample is expected to be measured using multiple analytical methods during one beam time because the measurement time will be drastically reduced. However, the use of conventional optical elements, of which the numerical aperture (NA) and working distance (WD) and so on are fixed, render the concept very inefficient or impossible because the most suitable beam differs depending on methods and samples. To overcome this problem, we have developed adaptive X-ray optical systems based on deformable mirrors capable of shaping X-ray beams with an optimized beam size, NA and WD for each experiment. In our previous research, we already achieved adaptive diffraction-limited X-ray focusing, in which the beam size was altered between 108 (165) and 560 (1434) nm in the vertical (horizontal) directions by controlling the NA of the focusing system[7]. Users often utilize collimated beams as well as focusing and divergent beams. Although they are usually formed with crystal collimators[8], refractive lenses[9] and total-reflection mirror[10,11] systems, they cannot produce adaptive collimations that can change the beam size. Furthermore, it is impossible to realize seamless switching between focused and collimated beams. In this research, we attempted the formation of two collimated beams with different sizes by utilizing the developed adaptive focusing system, with the aim of improving the versatility of the system.

Adaptive X-Ray Optics IV, edited by Stephen L. O'Dell, Ali M. Khounsary, Proc. of SPIE Vol. 9965, 996502 · © 2016 SPIE · CCC code: 0277-786X/16/$18 · doi: 10.1117/12.2238794

2. TWO-STAGE ADAPTIVE X-RAY OPTICAL SYSTEM

2.1 Piezoelectric deformable mirror

We developed deformable mirrors with a piezoelectric bimorph structure. The deformable mirrors consist of a quartz glass substrate, four piezoelectric actuators, and electrodes. Two piezoelectric actuators with 18 electrodes are attached to the face of the substrate and the other two actuators with a single electrode are attached to the back. The piezoelectric actuators can apply bending moment to the substrate in order to control local curvatures. The central region of the substrate was coated with a 100-nm thick molybdenum layer to be used as X-ray reflection area. The details are described elsewhere[7,12,13].

2.2 Two-stage adaptive Kirkpatrick-Baez mirror system

Figure 1 shows a one-dimensional schematic of the proposed adaptive X-ray optical system[7,14]. It consists of four deformable mirrors arranged in a two-stage Kirkpatrick-Baez (KB) configuration[15]. When a focused X-ray beam is generated, all the deformable mirrors are deformed into elliptical shape (Figure 1 (a)). The upstream elliptical mirror is designed to have foci at the X-ray source and at mid focus. The downstream elliptical mirror is designed to have foci at mid focus and final focus. The NA of the focusing system is varied to allow the beam size to be changed under the diffraction-limited condition by deforming the mirrors into an alternative elliptical shape that is designed to shift the mid focus position along the optical axis. This enables the NA to be changed without shifting the final focus position. On the other hand, when a collimated beam is generated, the downstream mirror is deformed into an ellipse with infinite focal length, in other words, a parabola (Figure 1 (b)). The size of the collimated beam can be varied by shifting the mid focus position in the same way. Consequently, the illumination area of the downstream mirrors varies according to the mid focus position, which leads to an adaptive change in the beam size of the collimated beam (Figure 1 (c)).

2.3 Deformation procedure for parallel beam

Fine adjustment of the deformation of the mirrors was achieved by employing the following procedure, which consisted of two parts: offline and online adjustment. The mirror shape was measured using an optical Fizeau interferometer (Verifire XPZ, Zygo Corp.) in the offline part. The figure error from the target shape was corrected by additionally deforming the mirror. This process was continued until each mirror was deformed into the target shape with an accuracy of 2 nm peak-to-valley. The applied voltage pattern that was finally applied to each electrode was recorded for the next step. Next, in the online adjustment, the mirrors were deformed by applying the same voltage pattern in the beamline. After this deformation, the mirrors had deformation errors of ~ 50 nm due to the hysteresis of the piezoelectric actuators. To finely correct the deformation errors, the applied voltages were adjusted on the basis of the mirror shapes determined with the X-ray pencil-beam scanning method[16,17]. This method involved the illumination of one section of the mirror surface by a small X-ray beam passing through a slit placed upstream of the mirror being tested. The reflected X-ray beam was detected using a beam monitor placed at an arbitrary position (e.g., the focal plane). This process was repeated until the entire effective area was scanned. Details of the mirror shape adjustment using the X-ray pencil-beam scanning method were as follows. First, the upstream mirrors were deformed into elliptical shapes using the beam monitor placed at the mid focus position. This process is the same as in our previous experiment where focused beams were generated[7]. However, the procedure for the downstream mirrors was quite different from that for the upstream mirrors. The parallelism of the collimated beam was measured with the X-ray pencil-beam scanning method, which involve the use of two beam monitors placed downstream of the downstream mirrors. Figure 2 shows a schematic of the system that was used to measure parallelism. The amounts of beam shift measured with the two beam monitors agree with each other during X-ray pencil beam scanning if the X-ray beam is completely collimated. Different beam shifts measured with the two beam monitors signify that the X-ray beam is not collimated. In this case, the parallelism error in each section of the beam is expressed as $\frac{\Delta z1-\Delta z2}{L}$, where Δz_1, Δz_2, and L are the amounts of beam shift detected with beam monitor 1 and 2, respectively, and the distance between the two beam monitors. The applied voltages were adjusted to minimize the distribution of the parallelism errors.

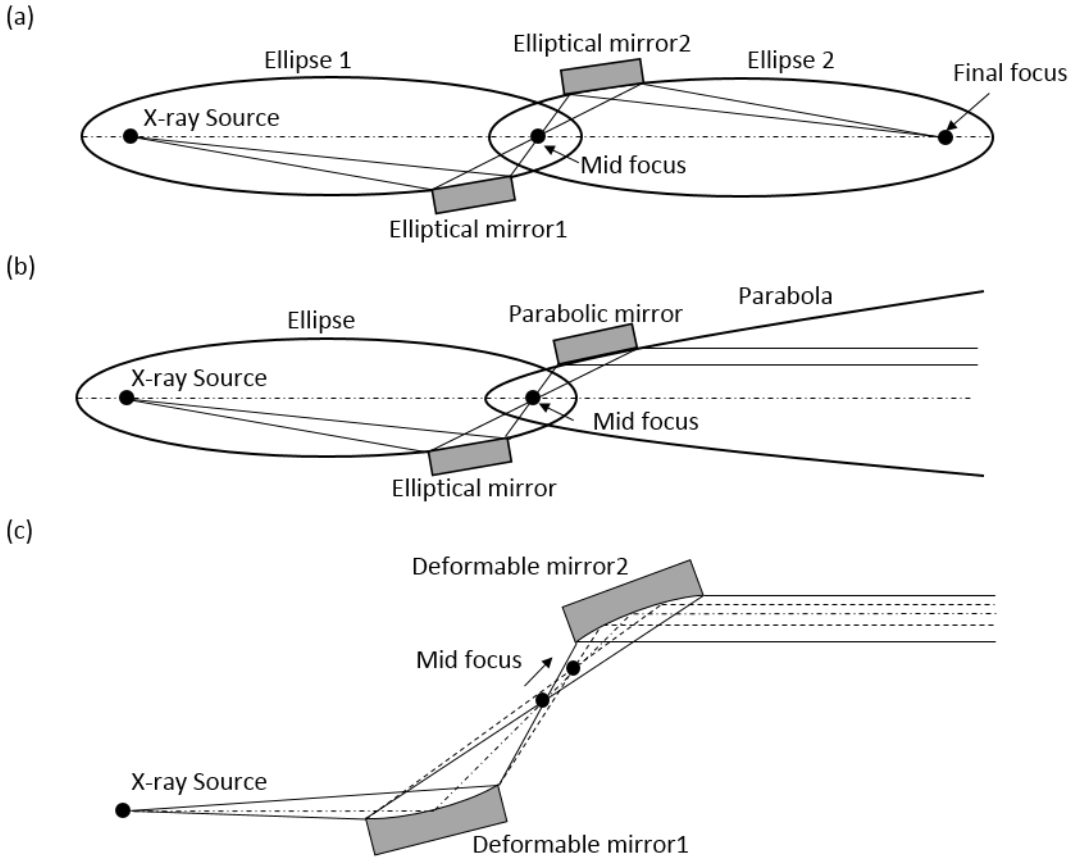

Figure 1. Schematic of the two-stage system for (a) focusing mode and (b) collimating mode. (c) Concept to change size of a collimated beam.

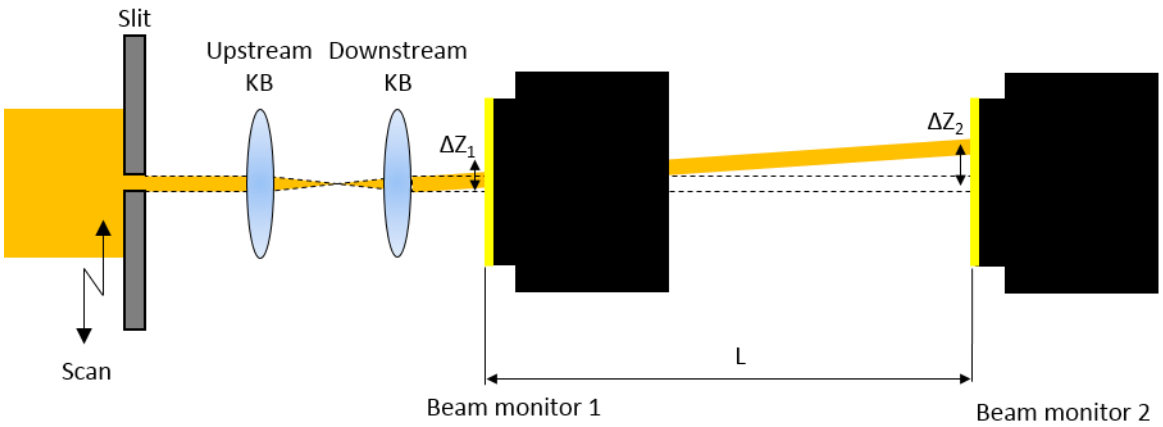

Figure 2. Schematic of the system to measure parallelism with the X-ray pencil-beam scanning method based on two beam monitors.

3. EXPERIMENT

3.1 Experimental setup

We performed an X-ray collimation test at BL29XUL (EH3) of SPring-8. Figure 3 shows a schematic and a photograph of the experimental setup. The distance between the upstream and downstream mirrors was 1240 mm and 1500 mm in the vertical and horizontal directions, respectively. X-ray energy of 10 keV was used in this experiment. For the X-ray pencil-beam scanning method, three specially developed beam monitors[7,13,18] were installed. The beam monitor 1 (BM1) was placed at mid focus to adjust the upstream mirrors. The beam monitor 2 (BM2) and the beam monitor 3 (BM3) were placed downstream of the downstream mirrors to measure the parallelism of the final beam. The distance between BM2 and BM3 was 2450 mm. In this experiment, two collimating modes (mode 1, 2), of which the parameters are shown in Table 1, was designed. In mode 1, the entire area of all the mirrors was used. On the other hand, in mode 2, 20% and 11 % of the entire area of the downstream horizontal and vertical mirrors was used, respectively. In mode 2, the mid focus was very close to the downstream mirrors, hence BM1 could not be placed at the mid focus position. Therefore, the upstream mirrors were not adjusted using the X-ray pencil-beam scanning method. The wavefront errors caused by the upstream mirrors were compensated when adjusting the shapes of the downstream mirrors while monitoring the wavefronts using BM2 and BM3, based on the concept of wavefront compensation.

3.2 Results

Figure 4 shows the observed intensity images (Figure 4 (a), (b)) and cross-sectional intensity profiles (Figure 4 (c), (d)) in mode 1. These results show that the beam sizes at BM1 and BM2 did not change in either direction. The measured beam size was 314 μm and 358 μm in the horizontal and vertical directions, respectively. Figure 4 (e) and (f) show the beam trajectories obtained with the X-ray pencil-beam scanning method at BM1 and BM2. In the X-ray pencil-beam scanning method, the silt width was set to 25 μm and the beam trajectory was measured at 12 points on the mirror surface. The standard deviation of the errors of the X-ray beam trajectory is 0.63 μm (0.71 μm) in the horizontal (vertical) directions, respectively, which corresponds to parallelism of 0.26 μrad and 0.29 μrad, respectively. Figure 5 shows the observed projection images (Figure 5 (a), (b)) and intensity profiles (Figure 5 (c), (d)) in mode 2. The measured beam size in the horizontal and vertical directions was 127 μm and 65 μm, respectively. Figure 5 (e) and (f) show the measured beam trajectory. In mode 2, the silt width was set to 20 μm and the beam trajectory was measured at 18 points on the mirror surface. The standard deviation of errors of the X-ray beam trajectory is 2.6 μm (1.9 μm) in the horizontal (vertical) directions, respectively. In the horizontal direction, one channel of the voltage supply units for the upstream mirror reached the upper limit value in terms of output. This is because the figure errors of the downstream mirror were corrected by deforming the upstream mirror. The amount of deformation of the upstream mirror became larger than we expected. Therefore, the wavefront errors were not compensated for completely. The standard deviation of the errors of the X-ray beam trajectory in the horizontal direction is 0.57 μm except for the first 3 points affected by the problem. The vertical and horizontal parallelism was 0.24 μrad and 0.8 μrad, respectively.

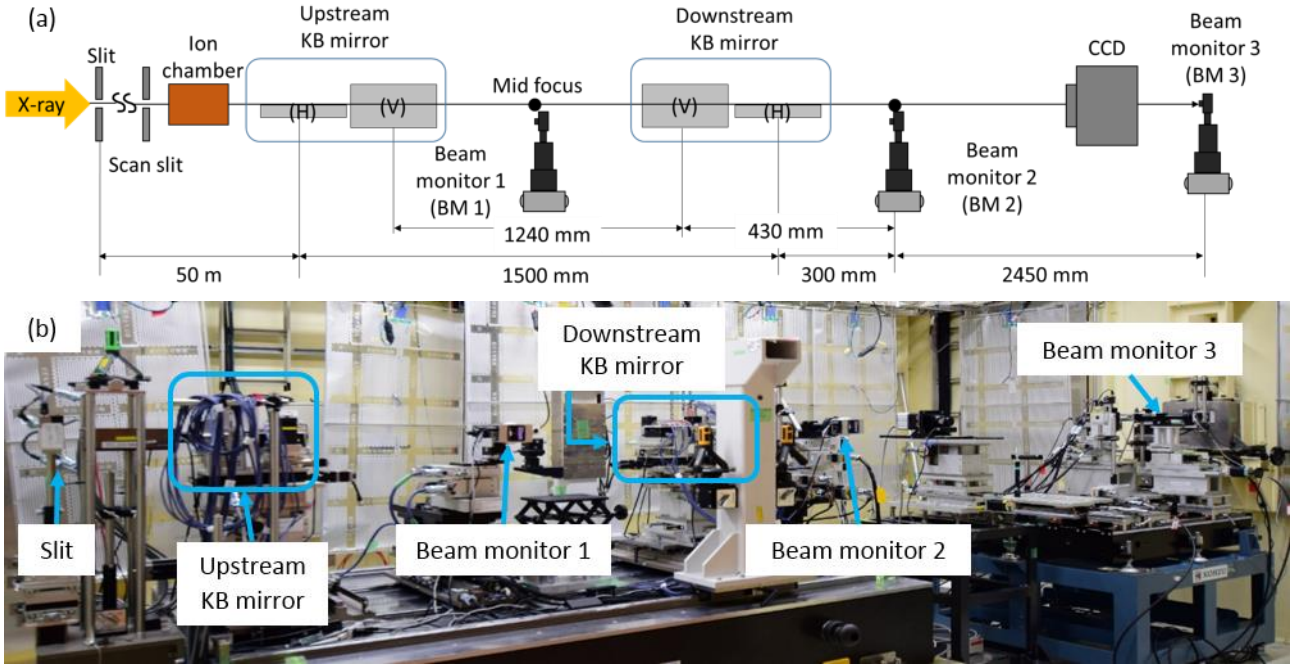

Figure 3. (a) Schematic (top view) and (b) photograph of the experimental setup for the two-stage adaptive KB mirror system

Table 1 Design parameters of the KB mirrors

	Horizontal	Vertical
Source – 1st mirror (mm) [a]	50000	50130
1st mirror – mid focus (mm)[a]		
Mode 1	750	620
Mode 2	1250	1120
1st mirror – 2nd mirror (mm)[a]	1500	1240
2nd mirror – Beam monitor 2 (mm)[a]	430	300
Beam monitor 2 – Beam monitor 3 (mm)	2450	2450
Grazing-incidence angle (mrad)[b]		
Upstream mirror	4.0	4.0
Downstream mirror	4.0	4.0

a Distance between centers of mirrors.
b At center of mirror

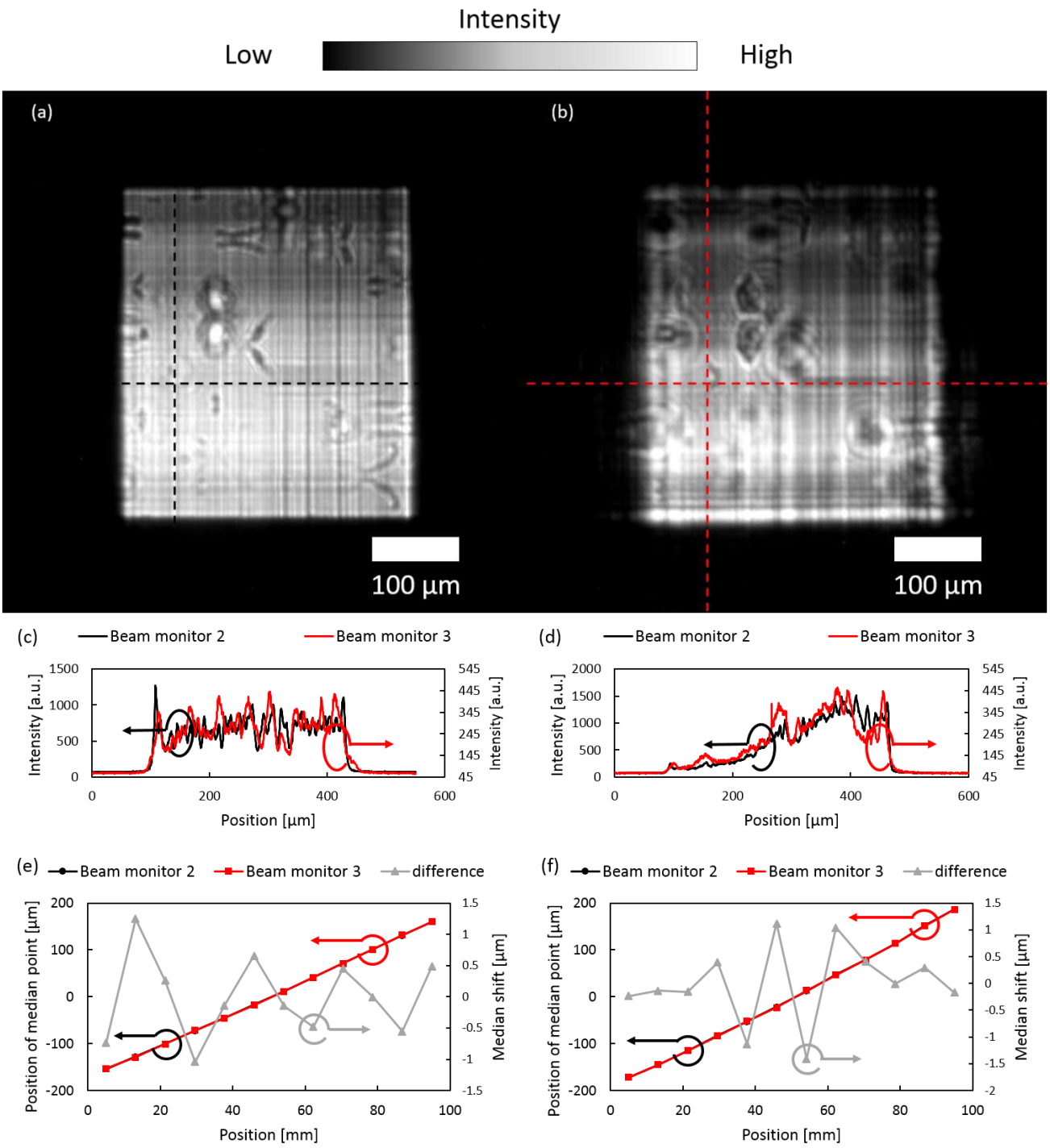

Figure 4. Experimental results in mode 1: X-ray beam images measured with (a) BM 2 and (b) BM3; intensity profiles (c) horizontal and (d) vertical through the dashed lines in (a) and (b) measured by BM 2 and BM 3; beam trajectory (e) vertical and (f) horizontal, and its errors measured with the X-ray pencil-beam scanning method. The vertical axis on the right represents the measured beam positions with both the beam monitors. The black and red lines are completely overlapped. The vertical axis on the left represents the trajectry errors between the results measured with the two beam monitors.

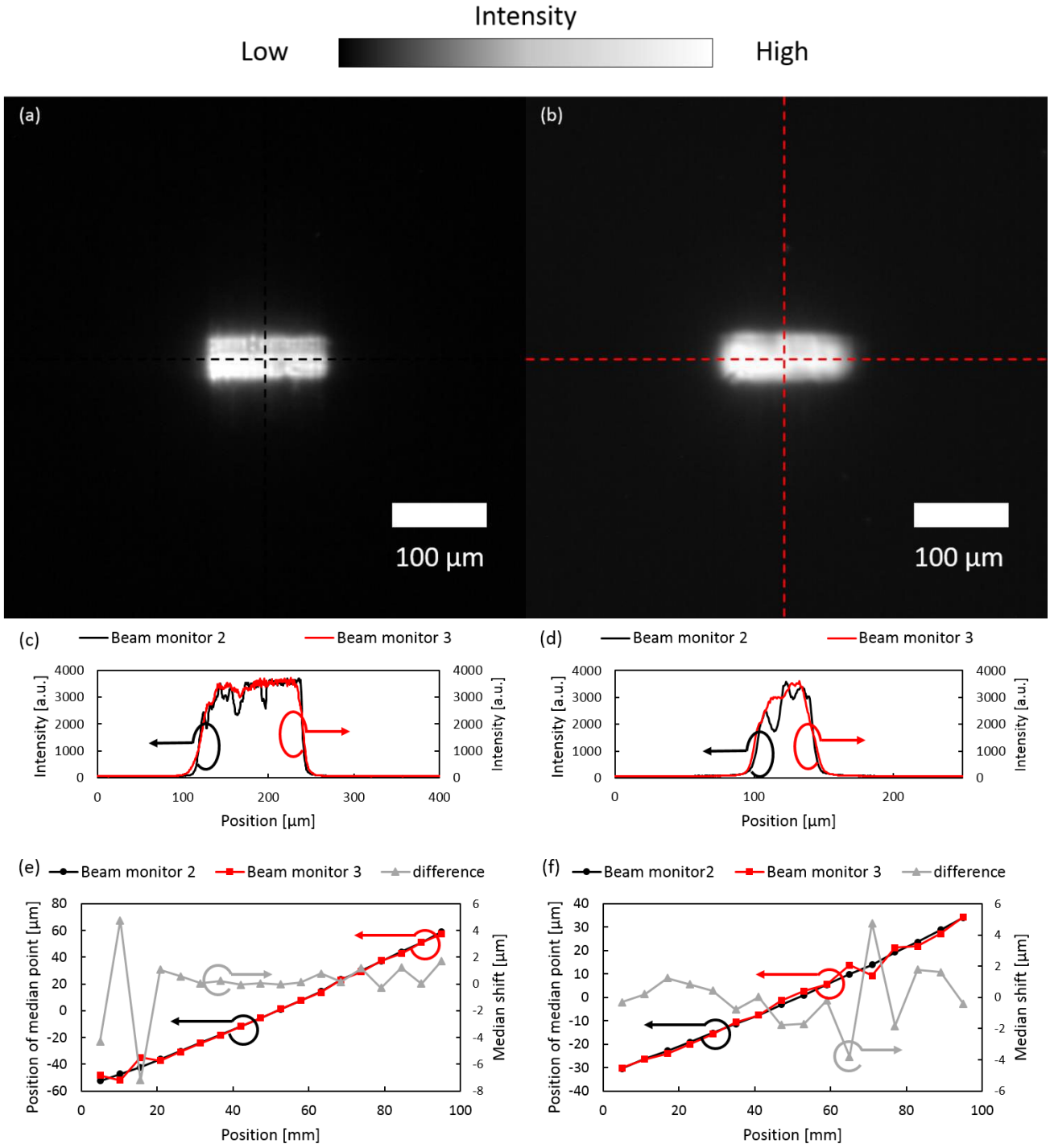

Figure 5. Experimental results in mode 2: X-ray beam images measured by (a) BM 2 and (b) BM3; the horizontal (c) and vertical (d) intensity profiles through the dashed lines in (a) and (b) were measured by BM 2 and BM 3. The vertical axes on the right and left represent the intensity of the CMOS camera. The vertical (e) and horizontal (f) beam trajectory and beam trajectory errors were measured by using the X-ray pencil-beam scanning method. The vertical axes on the left and right represent the trajectry errors of between the two beam monitors and the measured beam position of both beam monitors, respectively.

4. SUMMARY

We constructed a two-stage adaptive KB mirror system using four piezoelectric deformable mirrors. Using the system, we formed X-ray collimated beams at SPring-8. The use of the four deformable mirrors enabled us to achieve the formation of two collimated X-ray beams with different beam sizes with parallelism accuracy of ~ 1 μrad. We expect the adaptive X-ray optical systems to be useful for various multi-functional microscopes in advanced light sources, such as X-ray free electron lasers and ultimate storage rings.

ACKNOWLEDGMENTS

This research was supported by JSPS KAKENHI (Grant No. JP16H06358) and supported in part by JSPS KAKENHI (Grant Nos. JP23226004, JP26286077), JSPS Fellow (Grant No. 15J00656), CREST project of JST, the General Proposal Program of SACLA (Proposal Nos. 2015B8013, 2016A8010), and the JSPS Core-to-Core Program on the International Alliance for Material Science in Extreme States with High Power Laser and XFEL. The use of BL29XUL at SPring-8 was supported by RIKEN. We acknowledge the JTEC Corporation for assistance with mirror substrate processing.

REFERENCES

[1] C. G. Schroer, O. Kurapova, J. Patommel, P. Boye, J. Feldkamp, B. Lengeler, M. Burghammer, C. Riekel, L. Vincze, a. van der Hart, and M. Küchler, "Hard x-ray nanoprobe based on refractive x-ray lenses," Applied Physics Letters 87, 124103 (2005).

[2] A. Schropp, R. Hoppe, V. Meier, J. Patommel, F. Seiboth, Y. Ping, D. G. Hicks, M. A. Beckwith, G. W. Collins, A. Higginbotham, J. S. Wark, H. J. Lee, B. Nagler, E. C. Galtier, B. Arnold, U. Zastrau, J. B. Hastings, and C. G. Schroer, "Imaging Shock Waves in Diamond with Both High Temporal and Spatial Resolution at an XFEL.," Scientific. Reports, 5, 11089, (2015).

[3] H. Yan, V. Rose, D. Shu, E. Lima, H. C. Kang, R. Conley, C. Liu, N. Jahedi, A. T. Macrander, G. B. Stephenson, M. Holt, Y. S. Chu, M. Lu, and J. Maser, "Two dimensional hard x-ray nanofocusing with crossed multilayer Laue lenses.," Optics Express, 19 16 15069–76, (2011).

[4] H. Mimura, H. Yumoto, S. Matsuyama, Y. Sano, K. Yamamura, Y. Mori, M. Yabashi, Y. Nishino, K. Tamasaku, T. Ishikawa, and K. Yamauchi, "Efficient focusing of hard x rays to 25 nm by a total reflection mirror," Applied Physics Letters 90, 051903 (2007).

[5] H. Mimura, S. Handa, T. Kimura, H. Yumoto, D. Yamakawa, H. Yokoyama, S. Matsuyama, K. Inagaki, K. Yamamura, Y. Sano, K. Tamasaku, Y. Nishino, M. Yabashi, T. Ishikawa, and K. Yamauchi, "Breaking the 10 nm barrier in hard-X-ray focusing," Nature Physics 6, 122-125 (2009).

[6] "SPring-8-II Conceptual Design Report" http://rsc.riken.jp/pdf/SPring-8-II.pdf (November 2014) (accessed 10.09.16).

[7] S. Matsuyama, H. Nakamori, T. Goto, T. Kimura, K. P. Khakurel, Y. Kohmura, Y. Sano, M. Yabashi, T. Ishikawa, Y. Nishino, and K. Yamauchi, "Nearly diffraction-limited X-ray focusing with variable-numerical-aperture focusing optical system based on four deformable mirrors," Scientific. Reports, 6, 24801 (2016).

[8] S.Kikuta and K.Kohra, "X-Ray Crystal Collimators Using Successive Asymmetric Diffractions and Their Applications to Measurements of Diffraction Curves. I. General Considerations on Collimators" Journal of the Physical Society of Japan, 29 1322-1328 (1970)

[9] A. Q. R. Baron, Y. Kohmura, V. V Krishnamurthy, Y. V Shvyd'ko, and T. Ishikawa, "Beryllium and aluminium refractive collimators for synchrotron radiation," Journal of Synchrotron Radiation, 6, 5 953–956 (1999).

[10] I. Koshelev, R. Huang, T. Graber, M. Meron, J. L. Muir, W. Lavender, K. Battaile, A. M. Mulichak, and L. J. Keefe, "Focusing, collimation and flux throughput at the IMCA-CAT bending-magnet beamline at the Advanced Photon Source," Journal of Synchrotron Radiation, 16 5 647–657, (2009).

[11] D. Takei, Y. Kohmura, Y. Senba, H. Ohashi, K. Tamasaku, and T. Ishikawa, "X-ray collimation by the parabolic cylinder mirror in SPring-8/BL29XUL," Journal of Synchrotron Radiation, 23 1 158–162, (2016).

[12] H. Nakamori, S. Matsuyama, S. Imai, T. Kimura, Y. Sano, Y. Kohmura, K. Tamasaku, M. Yabashi, T. Ishikawa, and K. Yamauchi, "Experimental and simulation study of undesirable short-period deformation in piezoelectric deformable x-ray mirrors.," Review of Scientific Instruments, 83, 53701 (2012).
[13] T. Goto, H. Nakamori, T. Kimura, Y. Sano, Y. Kohmura, K. Tamasaku, M. Yabashi, T. Ishikawa, K. Yamauchi, and S. Matsuyama, "Hard X-ray nanofocusing using adaptive focusing optics based on piezoelectric deformable mirrors," Review of Scientific Instruments, 86, 43102 (2015).
[14] T. Kimura, S. Matsuyama, K. Yamauchi, and Y. Nishino, "Coherent x-ray zoom condenser lens for diffractive and scanning microscopy", Optics Express, 21, 8 9267–76 (2013).
[15] A. V Baez and P. Kirkpatrick, "Formation of Optical Images by X-Rays X-RAY OPTICS" Journal of the Optical Society of America, 6 1895 766–774, (1946).
[16] O. Hignette, A. Freund, and E. Chinchio, "Incoherent x-ray mirror surface metrology," Proc. SPIE, 3152, 188–199, (1997).
[17] J. Sutter, S. Alcock, and K. Sawhney, "In situ beamline analysis and correction of active optics", Journal of Synchrotron Radiation, 19, 6 960–8, (2012).
[18] T. Goto, S. Matsuyama, H. Nakamori, Y. Sano, Y. Kohmura, M. Yabashi, T. Ishikawa, and K. Yamauchi, "Simulation and Experimental Study of Wavefront Measurement Accuracy of the Pencil-Beam Method," Synchrotron Radiation News, 29, 4 32–36 (2016).